Segregation in mixtures of granular chains and spherical grains under vertical vibration

Xiaoxian Yuan,[1] Ning Zheng,[1,*] Qingfan Shi,[1] Gang Sun,[2] and Liangsheng Li[3,†]
[1]*School of Physics, Beijing Institute of Technology, Beijing 100081, China*
[2]*Institute of Physics, Chinese Academy of Sciences, Beijing 100190, China*
[3]*Science and Technology on Electromagnetic Scattering Laboratory, Beijing 100854, China*
(Received 16 October 2012; revised manuscript received 18 February 2013; published 10 April 2013)

We experimentally investigate segregation behaviors of binary granular mixtures consisting of granular chains and spherical grains with different interstitial media under vertical vibrations. A quantitative criterion is proposed to locate the boundaries between different vibrating phases. The water-immersed granular mixture exhibits two interesting types of segregation behaviors: chain-on-top and sandwich patterns. However, the phenomenon of sandwich segregation is absent for the air-immersed mixture. The topological differences of phase diagrams between two different environments indicate that the interstitial fluid plays an important role on the granular demixing. Additionally, the phase behaviors of mixtures for the different chain lengths show a not significant discrepancy. Finally, the vibrating thickness ratio determining the phase boundary characterizes the mixing extent of the granular bed. The estimated ratios for various chain lengths exhibit a monotonically decreasing dependence, when the vibration frequency increases.

DOI: 10.1103/PhysRevE.87.042203 PACS number(s): 45.70.Mg, 45.70.Qj, 83.80.Fg

I. INTRODUCTION

Phase segregation of mixtures is a broad spectrum of interesting problems in simple liquids [1], polarized fluids [2,3], polymer solutions [4,5], and granular systems [6–8]. At present most studies on granular segregation adopt spherical grains to investigate the mechanism, and the "Brazil nut effect" (BNE) or "reverse Brazil nut effect" (RBNE) is observed in binary granular beds subjected to vertical shaking [6–10]. Those segregated steady states are strongly sensitive to the viscosity of interstitial fluids [8,11] and the anisotropic shape of grains [12,13].

Recently, granular chains have received more and more attention from the scientific community because the chains capture some of the essential aspects of real polymers [14]. Not only are static and dynamic properties of granular chains worthwhile to study in themselves, but the analogy between macroscopic granular chains and microscopic molecular ones as well. Those designed granular chains might be used as an important simulation model in the field of polymers and could provide a possible way to uncover the physics that is experimentally inaccessible for polymers [15]. A similar behavior between jamming states of granular chains with glass states of polymers is illustrated by Zou *et al.*, who explored a three-dimensional packing structure of granular chains by x-ray tomography and found the inverse density of granular chains is analogous to the temperature of polymer solutions [16]. The effective stiffness of the packing of long chains increases with strain, where granular chains are constrained from significant rearrangements and form entangled loops [17]. When the entanglements of granular chains are absent, the strain stiffening effect disappears [18]. Furthermore, the formation of rigid semiloops in two-dimensional simulations indicates that the glass transition of polymers could be a kind of jamming transition [19]. And our experiments suggest that a two-dimensional statistical scaling behavior of packing collections of granular chains is in good accord with the theoretical expectation of polymers [20].

On the other hand, the two-dimensional dynamical properties of a vibrated granular chain without gravity can be described by Rouse model [21]. The radius of gyration and the structure factor of short chains can be matched by the random walk (RW) model, but the results of longer chains are well described by the self-avoiding random walk (SAW) model. However, the granular chains confined within a two-dimensional rotating tumbler during flow display a crossover transition, where shorter chains satisfy SAW statistics but longer chains follow the RW behavior [22]. Moreover, both first order and continuous phase transitions are observed in thin layer mixtures of poppy seeds and chains [23]. However, most of the researches on granular chains are mainly concerned with the analogy between the macroscopic granular chains and other microscopic systems such as polymers. The phase segregation for chain assembles or mixture to our knowledge is less involved, which is a new phenomenon of segregation for granular media.

In this paper we first observe segregation behaviors of water-immersed and air-immersed mixtures of granular chains and spherical grains under vertical vibrations in three dimensions, finding "chain-on-top" segregation and sandwich configurations. For the absence of sandwich or chain-on-bottom patterns in air, an analysis is presented to explain the underlying physics, indicating the importance of interstitial media in the granular segregation. We also propose a quantitative criterion to determine the boundaries of different phases and delineate the frequency and the acceleration strength, namely, f-Γ phase diagrams for different mixtures in which only the chain length varies, finding a similarity for all diagrams. Finally, we use the vibrating thickness ratio to characterize the mixing extent of the whole granular bed and show its dependence on the vibrating frequency.

*ningzheng@bit.edu.cn
†liliangsheng@gmail.com

II. EXPERIMENTAL METHODS

A. Air-immersed case

The air-immersed granular mixture that is confined in a glass cylinder with an inner diameter of 35 mm and a height of 140 mm consists of hollow alumina spheres and semirigid granular chains. The cylindrical container is mounted on a vibration platform attached to an electromechanical shaker which is used to excite vertical sinusoidal motion [see Fig. 1(a)], with the ratio of the horizontal vibration amplitude to the vertical vibration amplitude less than 3%. The granular chains are composed of hollow, steel beads with a diameter of 1.5 ± 0.1 mm and rods with the same material of an effective density 6.12 ± 0.05 g/cm^3. The maximum length of the rod connecting two adjacent beads is about 0.46 ± 0.02 mm, as shown in Fig. 1(b). The number of the beads required to form a smallest ring, $\xi = 10$, characterizes the stiffness of the granular chain, as Fig. 1(c) shows. The diameter of alumina grains ranges at 0.75 ± 0.05 mm, with an effective density 0.92 ± 0.06 g/cm^3.

The temperature and the humidity are maintained at 25 °C and within a range of 40%–50%, respectively. To minimize the side effect from the accumulation of electrostatic charges, an antielectrostatic surfactant is sprayed on the inner wall of the container evenly. Additionally, every 15 min a fresh mixture is replaced to avoid possible buildup of charges. Furthermore, this measure maintains the loss rate of alumina grains no more than 2%, since the parts of these grains fragment during long vibrations. Apart from such a mixture mentioned above, we also examine other binary combinations of the chains and glass ($\rho = 2.51$ g/cm^3), copper ($\rho = 8.90$ g/cm^3), and tungsten ($\rho = 19.35$ g/cm^3) spheres with the same size as alumina ones.

B. Water-immersed case

For the segregation experiment of the water-immersed granular mixture, we use another acrylic cylinder which has the same size as the glass one. The container is topped up firstly with distilled water slowly, and then a metal wire is used to expel bubbles on the inner wall. Small amounts of a surfactant, which have inappreciable effects on the final segregation, are used to remove the bubbles. After bubble-free water is obtained, we finally seal the water-immersed container with a rubber bung, as shown in Fig. 1(a). Here it is noteworthy that the top opening of the container is not sealed for the air-immersed case. Additionally, since the alumina spheres would suspend or float in water due to their smaller density ($\rho = 0.92$ g/cm^3), glass spheres ($\rho = 2.51$ g/cm^3) with the same size are used instead. Each volume of the granular components, in the proportion 50%:50%, used in the binary mixture is 15 ml for all data runs.

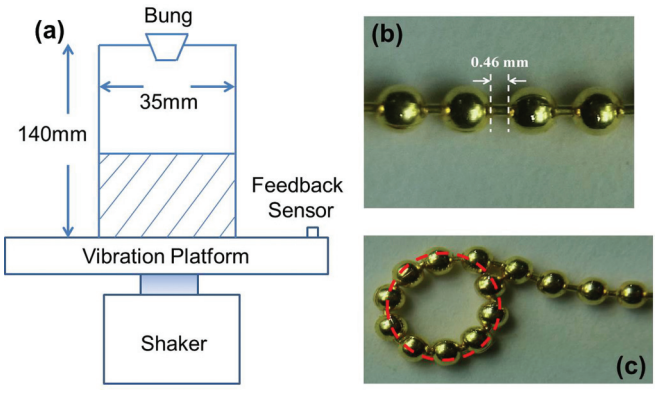

FIG. 1. (Color online) (a) Schematic diagram of the experimental apparatus, not to scale. The shadow area indicates the granular mixture. (b) Illustration of the length of the rod between two nearest beads on a semirigid chain. (c) The number of beads, $\xi = 10$, required to form a minimum loop is highlighted by the red dashed circle.

Before each experimental realization, both types of granular samples filled into the container using a funnel are mixed intimately. After all experimental conditions are well established, we control the shaker to vibrate at various frequencies f, from 20 to 200 Hz, and acceleration strength Γ, from 1 to 20. In general, the frequency f and the acceleration strength $\Gamma = A\omega^2/g$ are used as control parameters, where ω is the angular frequency of the vibration, A is the vibration amplitude, and g is the gravity acceleration. We record each stable, spatial configuration of the mixture by a high-resolution digital camera. It is worthy of note that all stable configurations are identified as a pattern that may be maintained 5 min or longer at given f and Γ.

Upon different vibrating conditions, several phases of the binary mixture appear, and the boundaries in a f-Γ phase diagram are firstly estimated by the visual inspection. In order to locate a boundary accurately, we propose a quantitative criterion which resorts to a measurement of the vibrating thickness ratio that is the ratio of the thickness of the pure glass (alumina) layer to whole granular bed. The data of thickness ratio in f-Γ plane are obtained from 20 snapshots for each experiment after the vibrating state reaches stability.

III. RESULTS AND DISCUSSION

A. Behaviors of the water-immersed granular mixture under vertical vibrations

Since the interstitial fluid plays an important role in granular separation in systems, we first investigate the water-immersed granular mixture. When Γ is not large enough, the components of the mixture migrate with extremely slow mobility. There is no any sign of segregation at an experimental time scale (at least for 20 min). Hence, the weak vibration status of mixture is observed as shown in Fig. 2. At the low-frequency region, when the external vibration starts and Γ is increased to fluidize the granular mixture, the chains in the bottom mixture are transported to the middle or middle-upper part of the granular bed by convection. Simultaneously, the glass grains in the top mixture sink downward and accumulate at the bottom of the container. Then chain-rich domains gradually merge and move up slowly, forming an upper layer. For a typical chain-on-top segregation, the interface between chain and glass grain layers is clear, and both layers are almost pure as shown in Fig. 2 inset. With continuously increasing Γ, the upper surface of the mixture is completely gasified, and the granular bed goes into a throwing status.

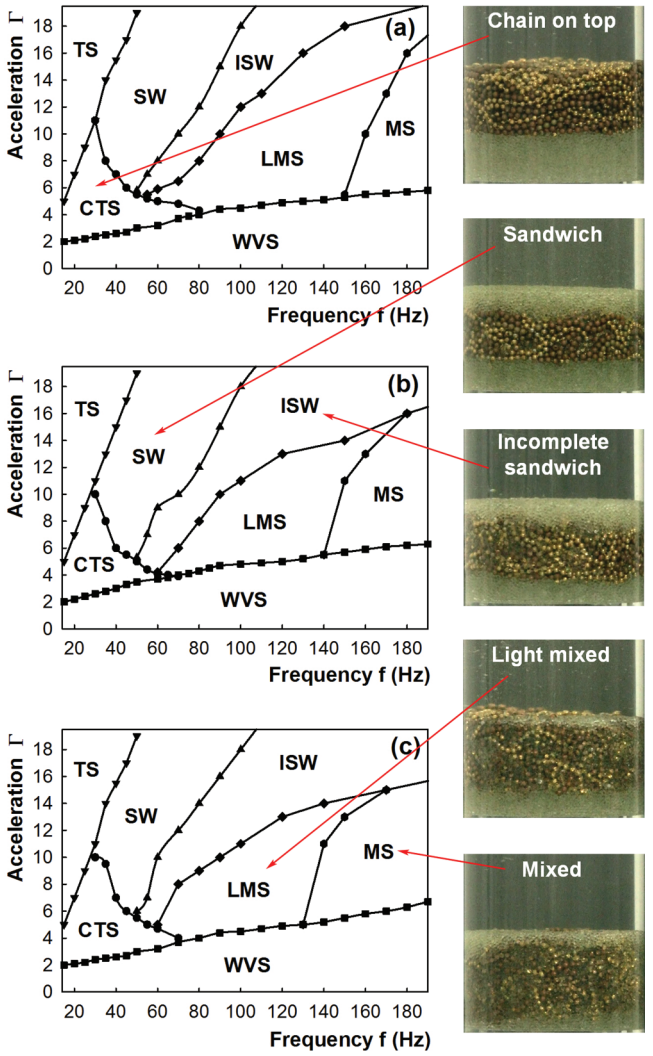

FIG. 2. (Color online) Schematic f-Γ phase diagrams for the water-immersed mixture consisting of glass spheres and granular chains with chain length (a) $N = 2$, (b) $N = 4$, and (c) $N = 8$, showing the regions described in the text. Solid lines are drawn to guide the eye. Region WVS: weak vibration status; CTS: chain-on-top segregation; LMS: light-mixed status; MS: mixed state; TS: throwing status; SW: sandwich segregation; ISW: incomplete sandwich segregation. Unless specified, the same regions in the following phase diagrams are represented by the same abbreviation in Figs. 4 and 5. Typical configurations shown by these photographs on the right: "chain on top" segregation, sandwich segregation, incomplete sandwich segregation, light-mixed status, and mixed state. The granular chains are gold, and the glass spheres are white.

Furthermore, a typical spatial structure of sandwich segregation in the middle frequency region is displayed in Fig. 2 inset, where the granular chains stay at the midlayer, and both top and bottom layers are occupied by glass spheres. However, the thicknesses of top and bottom glass layers are random even for given vibrating conditions. In the region of sandwich segregation, the amount of the glass spheres changes with vibration conditions, but less than 20%, estimated by visual inspection from the photographs after the cessation of vibration. When continuously increasing frequency, the interfaces of sandwich segregation become unstable, and the chain layer is doped by glass spheres. Then incomplete sandwich segregation appears, where top and bottom layers are still pure glass. We can incessantly raise frequency, and the glass grains of top layer keep diffusing into the chain layer until the top layer completely disappears. Then incomplete sandwich segregation is replaced by light-mixed status, where the interface between the glass bottom layer and the doped chain layer can still be observed, as shown by a photo inset in Fig. 2. With increasing frequency, the chain layer continuously absorbs the glass spheres of bottom layer, and the mixed state is restored.

In order to investigate the chain length dependence of the segregation effect, three granular combinations with different chain lengths, $N = 2$, 4, 8, are also adopted. The increase of the chain length enhances the aspect ratio of the granular chains, further differentiating the geometry from spherical grains. Those phase diagrams of the various short chains are topologically similar [see Figs. 2(a)–2(c)], which suggests that a short chain is analogous to a finite long rod but a soft one. When the length of a granular chain is far longer than the persistence length, new phases might emerge, such as the coil phase or the globule state of polymer solutions [24,25].

Next, a typical time dependence of the vibrating thickness ratio for two different behaviors is shown in Fig. 3(a), which indicates that the spatial conformation of the vibrating granular bed evolves for a while and finally reaches stability after 180 s for most situations. Therefore a long time (>180 s) needs to be expected before measuring this ratio, which is used to determine the boundary of different phases, as well as to quantify the mixing extent of the granular bed in the same phase region. According to the definition of the vibrating thickness ratio mentioned before, a better mixing extent is always associated with a smaller ratio.

In our experimental observation, the mixing extent of whole granular bed gradually enhances with the frequency. For this purpose the ratio as a function of the frequency at a given vibrating strength for the water-immersed mixture is shown in Fig. 3(b). When continuously increasing frequency, the ratio for all kinds of mixtures monotonically reduces and approaches vanishing. Additionally, it shows that the granular bed with longer chains seems to be inclined to mix if the same condition is given. It can be explained that the packing density of granular chains with free ends is a monotonically decreasing function of the chain length [16]. Longer chains therefore have more opportunities for bending or entanglement, producing more intrachain space to accommodate small glass spheres in the bed.

To quantitatively determine the boundary between phases, we suggest using the vibrating thickness ratio as a criterion. For example, the vibrating thickness ratio for a perfect chain-on-top conformation is about 0.5, and that for a complete mixed state is 0. We consider ratio 0.45 to be a reasonable value for the boundary of chain-on-top and the light mixed status as shown in Fig. 3(c), which is similar to the choice from Burtally *et al.* in BNE segregation [26]. In the same way, we prefer the ratio 0.15 as a reasonable value for the boundary between a mixed and the light mixed state. The same strategy is adopted to obtain the boundary between sandwich and incomplete sandwich status by this parameter. For instance, the ratio for

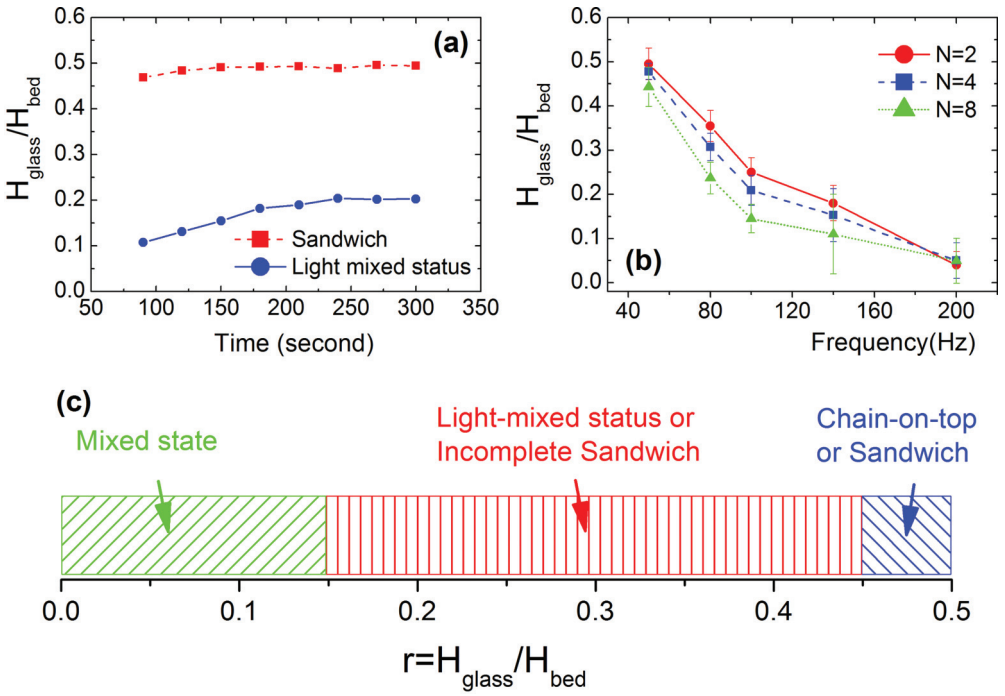

FIG. 3. (Color online) (a) Typical vibrating time dependence of vibrating volume ratio for two different vibrating behaviors; dashed red line for sandwich segregation, solid blue line for light mixed status, $N = 4$. (b) Vibrating volume ratio as a function of the frequency f at a given vibrating strength for different kinds of water-immersed mixture is shown. The solid red line indicates the chain length $N = 2$, dashed blue line for the chain length $N = 4$, and dotted green line for the chain length $N = 8$. All data points are averaged from 20 photos. (c) According to the definition of vibrating volume ratio in the text, a scale is plotted to indicate different vibrating phases. At both ends of the scale, the ranges of mixed states and segregated states are shown.

the pure sandwich conformation is about 0.5. If it is lower than 0.45, the region of the incomplete sandwich is thought to be approached.

B. Behaviors of the air-immersed granular mixture under vertical vibrations

1. *The mixture of granular chains and alumina spheres*

In order to compare the vibrating behaviors with different interstitial media and confirm the effect of interstitial media for segregation phases, only water is replaced by air without any other changes. In Fig. 4 the fundamental behavior in every region is similar to the water-immersed mixture, although some details differ to some extent. It is found that the motion of grains in the region of the light mixed status and of the throwing state are more violent compared with that in water. Chain-on-top segregation also has been observed in the low-frequency region. However, sandwich segregation fails to be found for the whole vibrating range. The Nottingham group [27] expressly stated that the effect of a fluid drag on granular materials scales as $\rho d^2/\eta$, where ρ indicates the density of the granular material, d, the diameter or the equivalent diameter of the grains, and η, the dynamic viscosity of the interstitial fluid. At room temperature, the dynamic viscosity of air is approximately 50 times smaller than that of water, so the diameter of the granular material is supposed to be about 7 times smaller than that in water for similar segregation.

In previous reports RBNE or sandwich patterns indeed occurred in a fine, air-immersed mixture consisting of binary grains, and a very distinct asymmetric heaping was often found during the formation of RBNE or sandwich patterns [10,26]. It is experimentally remarkable that the heaping is usually not predominant just for granular materials with large size. As is well known, the asymmetric heaping of granular grains can be attributed to the air effect [28]. If the ambient environment is highly evacuated, RBNE and sandwich segregation would be significantly suppressed or completely vanish, implying that the interstitial media in some cases affect the segregation decisively [11,29].

2. *The mixture of granular chains and other spheres*

In addition, other granular combinations including chains with different chain lengths and other kinds of spherical grains are also investigated to find the chain-on-bottom segregation or sandwich patterns. However, these segregation phases still fail to appear, and even chain-on-top segregation does not exist for the combinations of glass, copper, tungsten grains, and the chains. The typical phase diagram is shown as Fig. 5. Previous reports pointed out that if the size of granular grains is larger than 1–2 mm, the air effect will turn out to be negligible [11,27]. Considering the diameter of the steel beads on the chain is about 1.5 mm, and that of spherical grains is 0.7–0.8 mm in our experiment, we naturally assume that the reason for the absence of chain-on-bottom segregation or the sandwich pattern may result from the inefficiency of the interstitial air. Thus, chain-on-bottom segregation supposedly appears provided that the size of the granular chains can be

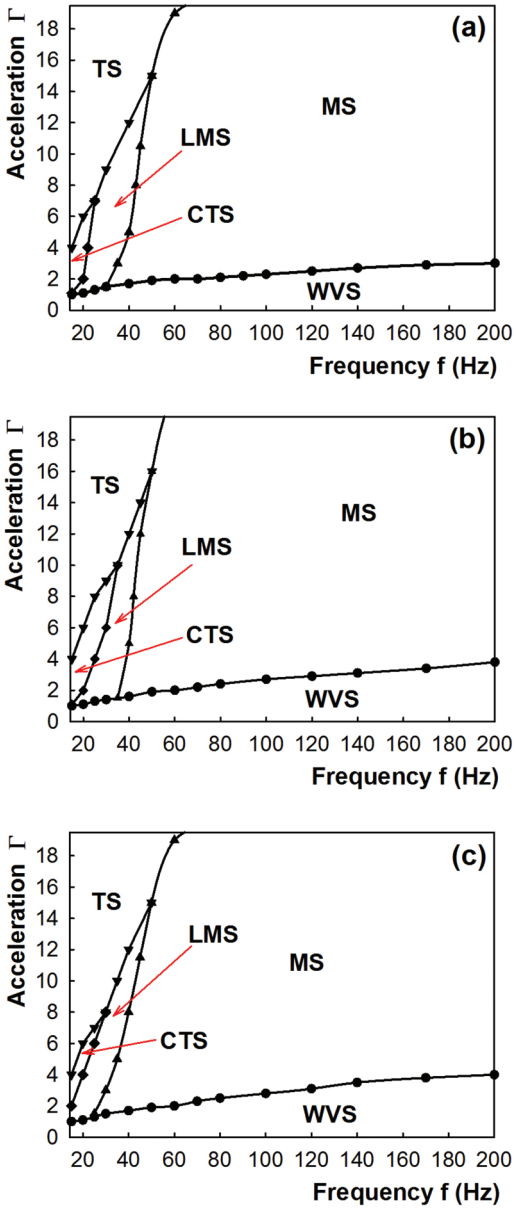

FIG. 4. (Color online) Schematic f-Γ phase diagrams for the air-immersed mixture consisting of alumina spheres and granular chains with chain length (a) $N = 2$, (b) $N = 4$, and (c) $N = 8$, showing the regions described in the text. Solid lines are drawn to guide the eye.

shrunk one order of magnitude. However, due to the machining difficulty, the chains with the ball diameter about 150–250 μm are incapable of being acquired.

Apart from a new segregation phase, it clearly shows that the segregation behaviors (region chain-on-top + pure sandwich segregation) in water are much more prevalent than those in air (only chain-on-top region), if comparing Fig. 2 with Fig. 4. Even if we compare the chain-on-top region, which is common in both phase diagrams, it evidently shows that this segregation region for the water-immersed case is much larger. These findings are not only valid for longer chains whose chain length $N = 8$, but also for other chains with chain length $N = 2$ and 4. From these experimental results, we can confirm that an appropriate interstitial fluid usually can take dual effects for

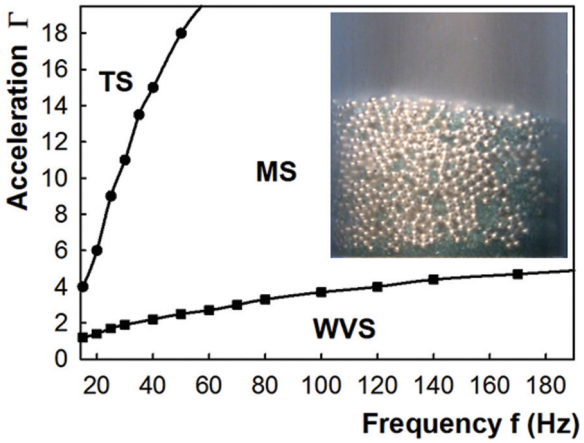

FIG. 5. (Color online) Schematic f-Γ phase diagram for the air-immersed mixture consisting of glass spheres and granular chains with chain length $N = 4$. Inset in the region MS: photograph for mixed state. The chains are identical with those in Figs. 2 and 4 except for the painting color. The granular chains are silver, and the glass spheres are dyed blue.

granular segregation of larger mixtures: on the one hand, the medium can create new segregation phenomenon (compare Fig. 2 with Fig. 5); on the other hand, the segregation extent can be notably improved.

IV. SUMMARY

In conclusion, first we experimentally investigate the segregation behaviors of the water-immersed mixture and plot f-Γ phase diagrams in which different vibrating behaviors are detailed. In addition, we define a vibrating thickness ratio to distinguish boundaries of different phases and to characterize the mixing extent for the whole granular bed. It is found that this parameter reduces monotonically with the vibrating frequency, suggesting that the mixing extent would be enhanced. We also studied the segregation behaviors of granular combinations with different chain lengths, finding that their phase diagrams appear to have a close similarity fundamentally. To compare the vibrating behaviors and investigate the effect of interstitial media for such a binary mixture with large grains, the surrounding fluid was replaced by air, which had a different viscosity. The variety of vibrating phases is reduced for an air-immersed mixture, where we observed only pure chain-on-top segregation, but failed to find the sandwich configuration. An explanation is presented to account for the difference between two fluid-immersed cases, further confirming that one of the mechanisms for the segregation of the granular mixture with a large size can be attributed to the effect of the interstitial fluid on the granular motion.

Future work aims to computationally reproduce the experimental results as observed in the laboratory. In addition, we did not find the ordering of the granular chains in the segregation. We prepare to design some constraints to find such ordering under vertical vibrations, and hope to propose an analogy with the structural behaviors of liquid crystal.

ACKNOWLEDGMENTS

We appreciate Pingping Wen for designing and building the watertight container. The work was supported by the National Natural Science Foundation of China (Grants No. 11104013, 10975014, and 10875166) and Excellent Young Scholars Research Fund of the Beijing Institute of Technology.

[1] T. Coussaert and M. Baus, Phys. Rev. Lett. **79**, 1881 (1997).
[2] X. S. Chen, M. Kasch, and F. Forstmann, Phys. Rev. Lett. **67**, 2674 (1991).
[3] L. S. Li, L. Li, and X. S. Chen, Commun. Theor. Phys. **51**, 287 (2009).
[4] J. L. Jacobsen, Phys. Rev. E **82**, 051802 (2010).
[5] M. Schmidt, H. Löwen, J. M. Brader, and R. Evans, Phys. Rev. Lett. **85**, 1934 (2000).
[6] J. B. Knight, H. M. Jaeger, and S. R. Nagel, Phys. Rev. Lett. **70**, 3728 (1993).
[7] D. A. Huerta and J. C. Ruiz-Suarez, Phys. Rev. Lett. **92**, 114301 (2004).
[8] N. Burtally, P. J. King, and M. R. Swift, Science **295**, 1877 (2002).
[9] D. C. Hong, P. V. Quinn, and S. Luding, Phys. Rev. Lett. **86**, 3423 (2001).
[10] S. S. Du, Q. F. Shi, G Sun, L. S. Li, and N. Zheng, Phys. Rev. E **84**, 041307 (2011).
[11] M. Klein, L. L. Tsai, M. S. Rosen, T. Pavlin, D. Candela, and R. L. Walsworth, Phys. Rev. E **74**, 010301(R) (2006).
[12] C. R. A. Abreu, F. W. Tavares, and M. Castier, Powder Technol. **134**, 167 (2003).
[13] R. Caulkin, X. Jia, M. Fairweather, and R. A. Williams, Phys. Rev. E **81**, 051302 (2010).
[14] C. J. Olson Reichhardt and L. M. Lopatina, Science **326**, 374 (2009).
[15] E. Ben-Naim, Z. A. Daya, P. Vorobieff, and R. E. Ecke, Phys. Rev. Lett. **86**, 1414 (2001).
[16] L. N. Zou, X. Cheng, M. L. Rivers, H. M. Jaeger, and S. R. Nagel, Science **326**, 408 (2009).
[17] E. Brown, A. Nasto, A. G. Athanassiadis, and H. M. Jaeger, Phys. Rev. Lett. **108**, 108302 (2012).
[18] I. Regev and C. Reichhardt, Phys. Rev. E **87**, 020201(R) (2013).
[19] L. M. Lopatina, C. J. Olson Reichhardt, and C. Reichhardt, Phys. Rev. E **84**, 011303 (2011).
[20] P. P. Wen, N. Zheng, L. S. Li, H. Li, G. Sun, and Q. F. Shi, Phys. Rev. E **85**, 031301 (2012).
[21] K. Safford, Y. Kantor, M. Kardar, and A. Kudrolli, Phys. Rev. E **79**, 061304 (2009).
[22] X. Ulrich, E. Fried, and A. Q. Shen, Phys. Rev. E **80**, 030301(R) (2009).
[23] T. Sykes and T. Mullin, Phys. Rev. E **80**, 051301 (2009).
[24] R. Du, A. Y. Grosberg, and T. Tanaka, Phys. Rev. Lett. **83**, 4670 (1999).
[25] T. Palberg, A. Stipp, and E. Bartsch, Phys. Rev. Lett. **102**, 038302 (2009).
[26] N. Burtally, P. J. King, M. R. Swift, and M. C. Leaper, Gran. Matt. **5**, 57 (2003).
[27] M. C. Leaper, A. J. Smith, M. R. Swift, P. J. King, H. E. Webster, N. J. Miles, and S. W. Kingman, Gran. Matt. **7**, 57 (2005).
[28] M. Faraday, Philos. Trans. R. Soc. London **121**, 299 (1831); H. K. Pak, E. van Doorn, and R. P. Behringer, Phys. Rev. Lett. **74**, 4643 (1995); R. P. Behringer, E. van Doorn, R. R. Hartley, and H. K. Pak, Gran. Matt. **4**, 9 (2002); H. J. van Gerner, G. A. Caballero-Robledo, D. van der Meer, K. van der Weele, and M. A. van der Hoe, Phys. Rev. Lett. **103**, 028001 (2009).
[29] M. E. Möbius, X. Cheng, P. Eshuis, G. S. Karczmar, S. R. Nagel, and H. M. Jaeger, Phys. Rev. E **72**, 011304 (2005).